JOURNAL OF APPLIED PHYSICS VOLUME 93, NUMBER 11 1 JUNE 2003

Effect of crystal orientation on the implant profile of 60 keV Al into 4H-SiC crystals

J. Wong-Leung[a)]
Department of Electronic Materials Engineering, Research School of Physical Sciences and Engineering, Australian National University, Canberra, ACT 0200, Australia

M. S. Janson and B. G. Svensson[b)]
Royal Institute of Technology, Solid State Electronics, Electrum 229, S-164 40 Kista-Stockholm, Sweden

(Received 7 February 2003; accepted 6 March 2003)

4H-SiC wafers of orientations (0001) and $(11\bar{2}0)$ were implanted with 60 keV Al^- in different major axial, planar, and low symmetry (''random'') directions to ascertain the degree of channeling and to determine the optimum tilt conditions for ion implantation. Significant channeling was observed for all axial directions with the $[11\bar{2}0]$ channel exhibiting the deepest channeling with a maximum penetration depth 45 times greater than the projected range of the random implants. Significant channeling was observed for the $\{11\bar{2}0\}$ and especially the {0001} planar channels while the implants in the $\{10\bar{1}0\}$ planar channels did not differ from the corresponding random implants. To minimize channeling in (0001) crystals, our results show that beam alignment normal to the surface is advisable for off-axis (0001) wafers with the miscut toward $\langle 11\bar{2}0\rangle$, while tilting of the wafer is necessary when the miscut is toward $\langle 10\bar{1}0\rangle$. For the $(11\bar{2}0)$ material, channeling can be minimized by a tilt of $\gtrsim 10°$ toward the [0001] direction. © *2003 American Institute of Physics.*
[DOI: 10.1063/1.1569972]

I. INTRODUCTION

Silicon carbide is a promising wide band gap semiconductor for applications in high power, high frequency, and high temperature devices. One of the key challenges in silicon carbide research will be the implementation of ion implantation processing in device fabrication. Commercial (0001) wafers are generally offered with a miscut of $3.5°-8.5°$ to facilitate epitaxial growth. Currently, the off-axis miscut is either toward the $\langle 11\bar{2}0\rangle$ or $\langle 10\bar{1}0\rangle$ directions depending on the supplier.[1,2] Thus, implanting normal to the wafer surface is equivalent to a tilt of the crystal in the $\{10\bar{1}0\}$ or $\{11\bar{2}0\}$ plane, respectively. It is unclear whether implantation normal to the wafer surfaces of these configurations is adequate for minimizing channeling effects in (0001) 4H-SiC wafers. A few studies have been directed to the effect of channeling in the ion implantation of silicon carbide in (0001) 6H-SiC crystals, both theoretical and experimental.[3–8] However, the effect of the miscut in a planar orientation on channeling is unclear. Further, for lateral metal–oxide-field effect transistors fabricated on $(11\bar{2}0)$ 4H-SiC crystals, a substantially enhanced electron mobility in the inversion channel compared to that on (0001) wafers has been reported.[9] Yet, there has not been any reports regarding ion channeling in conjunction with ion implantation of $(11\bar{2}0)$ SiC wafers, a direction with a very open channel structure. In this study, we report on the effect of crystal orientation on the implantation profiles of Al in both (0001) and $(11\bar{2}0)$ oriented 4H-SiC wafers.

II. EXPERIMENT

Implantation of 60 keV Al^- was performed at room temperature into 4H-SiC *n*-type substrates from Cree Inc. through a circular aperture of 4 mm in diameter. The beam divergence was $\leq 0.08°$. Alignment of the crystals was performed by registering the backscattering yield of a 1.46 MeV H^+ beam using a solid state detector mounted close to the incident beam direction. The orientation was determined by noting the angular dips (i.e., decrease in current with change of tilt) associated with the planes orthogonal to the crystal direction of the sample. Wafers of two different orientations were used: (0001) with an off-axis miscut of about 8° toward $[11\bar{2}0]$ and on-axis $(11\bar{2}0)$. Simulations were performed using a binary collision approximation (BCA) program code called SIIMPL[10] to predict implantation profiles for various tilt angles along the major planes close to two main wafer orientations namely the (0001) and the $(11\bar{2}0)$.

For the (0001) wafers, the samples were mounted on a tilt-rotate two axis goniometer with the rotation axis close to the incident beam direction and the tilt axis in the vertical axis. The three $\{11\bar{2}0\}$ planes orthogonal to the (0001) plane could be mapped at 60° to each other by the large angular dips recorded in the backscattered signal. Each of the three $\{10\bar{1}0\}$ planes, also orthogonal to the (0001) and halfway between two adjacent $\{11\bar{2}0\}$ planes, was registered as

a)Electronic mail: jwl109@rsphysse.anu.edu.au
b)Also at: University of Oslo, Physics Department, P.B. 1048 Blindern, Oslo, N-0316, Norway.

Downloaded 10 Oct 2007 to 150.203.178.60. Redistribution subject to AIP license or copyright, see http://jap.aip.org/jap/copyright.jsp

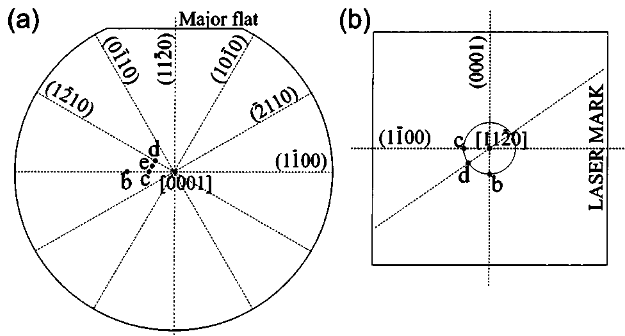

FIG. 1. Stereogram showing the geometry used for the different implants in the (a) (0001) and (b) $(11\bar{2}0)$ wafers.

smaller dips in the backscattered signal compared to the $\{11\bar{2}0\}$ planes. This is consistent with the fact that the $\langle 10\bar{1}0\rangle$ direction has less open channels compared to the $\langle 11\bar{2}0\rangle$, the latter being equivalent to the $\langle 110\rangle$ channels in the cubic silicon lattice. The location of alternating $(11\bar{2}0)$ and $(10\bar{1}0)$ planes at every 30° made us choose a plane in between adjacent $(11\bar{2}0)$ and $(10\bar{1}0)$ planes as the "random" plane. The convention used for the crystallographic planes with respect to wafer orientation and major flat is illustrated in Fig. 1(a). Five different directions were chosen for implantation, namely: (a) the [0001] direction, (b) the $[11\bar{2}3]$ direction, 17° tilt in the $(1\bar{1}00)$ plane, (c) 9° off [0001] in the $(1\bar{1}00)$ plane, (d) 8° off [0001] in $(1\bar{2}10)$ plane, and (e) 8° off [0001] halfway between $(1\bar{1}00)$ and $(1\bar{2}10)$ planes. The latter implant will be referred to as the "(0001) random" implant. These directions are clearly indicated in the form of a stereogram in Fig. 1(a).

The $(11\bar{2}0)$ wafers have two orthogonal planes to this direction, namely the (0001) and $(1\bar{1}00)$ planes and the convention used for the geometry of the sample with respect to the $[11\bar{2}0]$ wafer normal and the laser mark is illustrated in Fig. 1(b). For this orientation, we observed significant dips in the backscattering signal with the (0001) plane while minor dips of about 25% was observed for the $(1\bar{1}00)$ plane. For the $(11\bar{2}0)$ wafers, a double tilt goniometer was used to align the sample to four chosen orientations: (a) $[11\bar{2}0]$ direction, (b) 10° tilt in the (0001) plane, (c) 10° tilt in the $(1\bar{1}00)$ plane, and (d) 10° tilt in the plane between the (0001) and $(1\bar{1}00)$ planes (forming an angle of 55° with the (0001) plane) later referred to as the "$(11\bar{2}0)$ random" implant. These orientations are clearly labeled in Fig. 1(b).

After alignment, the H beam was substituted to 60 keV Al^- and the samples were implanted to a nominal dose of 5×10^{13} cm^{-2}. The use of an unscanned beam resulted in a variation of implanted dose over the sample surface, ranging from 5×10^{12} to 1.6×10^{14} cm^{-2}. Depth profiles of the implanted Al was obtained by secondary ion mass spectrometry (SIMS) using a Cameca ims $4f$ instrument. The SIMS profiles were determined using a primary sputtering beam of 8 keV $^{32}(O_2)^+$ ions rastered over an area of 80×80 μm^2. The detected Al^+ ions were collected from an area, 8 μm in

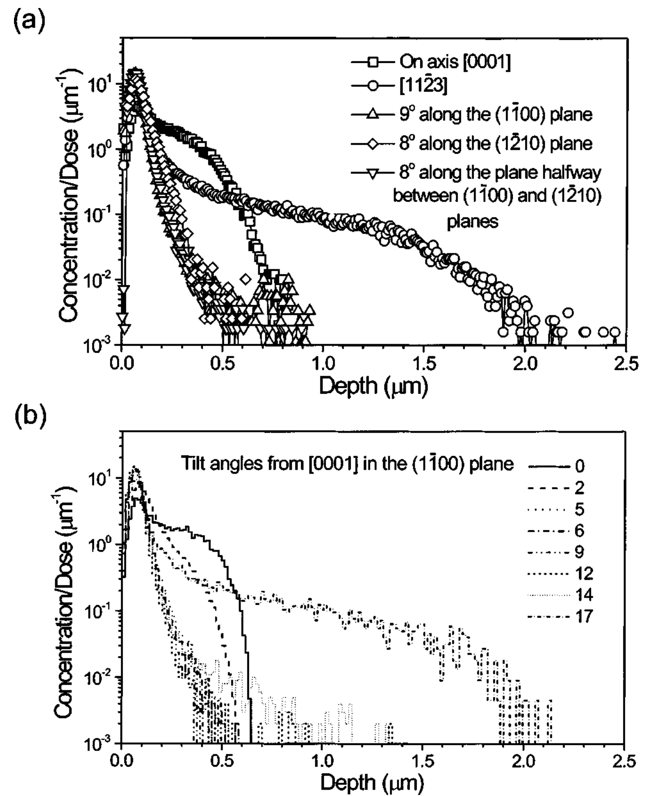

FIG. 2. (a) SIMS profiles of 60 keV Al implanted samples tilted at various angles in planes described around the [0001] axis (b) Monte Carlo simulated profiles of 60 keV Al implantations comparing various tilt angles from the [0001] axis in the $(1\bar{1}00)$ plane.

diameter, in the center of the sputtered crater. Since the implanted dose over the 8 μm analyzed area was estimated to be constant within the experimental accuracy ($\sim$10%), SIMS analysis could be used to determine the implantation distribution locally. In this way profiles with varying implantation dose could be obtained from each sample. The damage resulting from the focused H beam ($\leqslant$2 mm in diameter) during alignment was visible as a dark spot and that area could therefore be avoided in the SIMS measurements. Sample charging during SIMS analysis was a main concern with these samples, most likely due to damage caused by the intense H beam during alignment. To compensate for sample charging, 9 keV electrons were flooded over the sputtered area during SIMS measurements.

III. RESULTS AND DISCUSSION

Figure 2(a) shows the Al profiles of the various implants in (0001) SiC wafers. For easier comparison, the SIMS profiles have been normalized with respect to their respective doses. The individual profiles chosen for this plot represent doses below those where dose dependence effects were observed as will be discussed later. The on-axis implant shows a very broad profile in agreement with previous [0001] implant profiles in 6H-SiC.[5,8] Furthermore, the $[11\bar{2}3]$ channel gives a more than two times deeper profile than the [0001] channel, but the fraction of channeled ions is smaller. A tilt of 8° in the $(11\bar{2}0)$ plane shows a slight, but significant

Downloaded 10 Oct 2007 to 150.203.178.60. Redistribution subject to AIP license or copyright, see http://jap.aip.org/jap/copyright.jsp

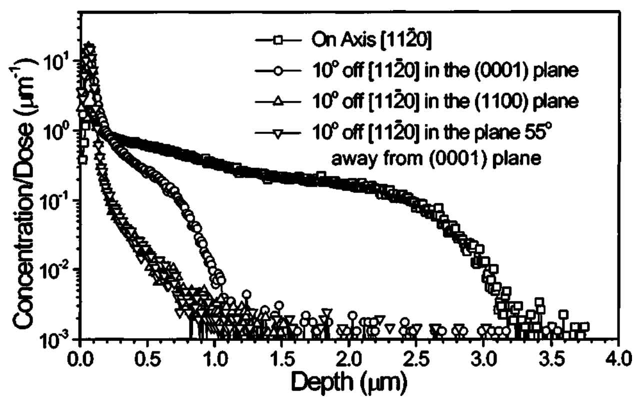

FIG. 3. SIMS profiles of 60 keV Al implanted samples tilted at various angles in planes around the [11$\bar{2}$0] axis.

broadening of profile compared to the (0001) random sample, while the sample implanted at an angle of 9° in the (1$\bar{1}$00) plane shows no trace of additional channeling in that plane.

Computer simulations within the BCA[10] were carried out at various tilt angles around the [0001] direction and Fig. 2(b) shows the simulated Al distributions for different tilt angles in the (1$\bar{1}$00) plane. The simulated implants are in good agreement with the experimental profiles and also show that the profile shape is rather insensitive on the tilt angle for tilts between 5° and 12°. The profiles of these implants also coincided with the simulated (0001) random implant (not shown), in agreement with the experimental result. In further agreement with the experimental SIMS profiles, the [11$\bar{2}$3] axis implant displayed a deeper channeling tail compared to the channeling tail observed for the on-axis [0001] implant. Previously, Albertazzi and Lulli[3] reported that Monte Carlo simulation of ion implantation in 6H-SiC showed a peak in the degree of channeling at a tilt angle of ~12° in the (10$\bar{1}$0) plane which is incidentally close to the [11$\bar{2}$3] axial direction in 6H-SiC crystals (11.6° tilt in the {10$\bar{1}$0} plane). This is in agreement with our simulations (not shown)[10] and implies that the [11$\bar{2}$3] channel in 6H-SiC is an equally important channeling direction as in 4H-SiC.

The normalized profiles of the (dose-independent) implantations in the (11$\bar{2}$0) material are shown in Fig. 3. For this crystal orientation, the on-axis [11$\bar{2}$0] direction showed a significantly broader profile compared to the on axis [0001] implant [compare square symbols in Figs. 2(a) and 3], with a maximum penetration 45 times deeper than the projected range of the corresponding random implant. Around this axis, significant planar channeling is observed in the sample tilted at 10° in the (0001) plane. In contrast, the sample tilted at 10° in the (1$\bar{1}$00) plane showed an identical Al distribution to the (11$\bar{2}$0) random implant.

Our results clearly show that for (0001) oriented 4H-SiC crystals with an 8° miscut toward ⟨11$\bar{2}$0⟩, implantation normal to the wafer surface is sufficient to minimize channeling. This is not the case for off-axis (0001) material cut toward ⟨10$\bar{1}$0⟩, which should be implanted with a tilt of the wafer relative to the beam to avoid planar channeling. It should be noted that these recommendations are only valid for 4H-SiC since (0001) 6H-SiC is normally cut with a smaller off-axis angle of 3.5°. Our simulations show that this tilt angle is not large enough to minimize channeling in the (0001) channel, at least not for 60 keV Al. Furthermore, the choice of tilt angle is a little more delicate for 6H- than for 4H-SiC since the [11$\bar{2}$3] axial channel is much closer to [0001] in 6H-SiC (11.6° in the {10$\bar{1}$0} plane). With regards to on-axis (11$\bar{2}$0) 4H-SiC material, implantation normal to the wafer or with a tilt of the wafer toward the [1$\bar{1}$00] direction is not advisable. Instead a tilt toward [0001], or in some plane between the (1$\bar{1}$00) and (0001) planes, should be used. Our simulations further suggest that a tilt angle of at least 10° should be used for (11$\bar{2}$0) substrates to minimize the channeling in the wide [11$\bar{2}$0] axial-channel.

As mentioned earlier, implantations with varying dose were obtained from each implant. Figure 4 shows the variation of Al distribution with implanted dose for the [0001], the 9° off [0001] in the (1$\bar{1}$00), and [11$\bar{2}$3] implantations. In Fig. 4(a), the two lower doses showed identical Al distributions if normalized with the dose. For higher Al doses, the Al distribution at the end of the channeling tail saturated at the same level with a larger fraction of the implanted Al located around the depth of the projected range for a corresponding random implant. This is consistent with previous reports[5] and is attributed to dechanneling at interstitial type defects created by the preceding ions. For the (0001) wafers, a clear dose dependence was observed for sample implanted either in the [0001] and [11$\bar{2}$3] axial channels, Figs. 4(a) and 4(c), respectively, or in the (11$\bar{2}$0) planar channel implantations while the remaining implants exhibited no dose dependence for the studied dose range. We note that the remaining implants displayed distributions close to the Al random profile. This behavior is exemplified in Fig. 4(b) for the implantation 9° off [0001] in the (10$\bar{1}$0) plane. There is a distinct variability on the threshold dose below which no dose dependence is observed but typically, a dose of $\sim 1\times10^{13}$ cm^{-2} is low enough to avoid a dose effect in all of the studied cases.

In contrast to the implants performed in the (0001) crystals, we did not observe any significant dose dependence for most of the implants in the (11$\bar{2}$0) wafer. However, the implant distribution for the implants in the (11$\bar{2}$0) wafers are relatively broader compared to the implants in the (0001) wafers. This in itself results in a dilution of the damage and can therefore explain a higher threshold dose where the dose dependence is observed. Furthermore, [0001] on-axis implants have been shown to result in significantly lower damage concentration[5] compared to random implants, since a greater part of the ion energy is dissipated in electronic stopping for channeled ions. Thus, a lower damage buildup in the [11$\bar{2}$0] wider channel may explain a higher threshold dose for dose dependent effects in the implants performed in the (11$\bar{2}$0) material. For these reasons, it is difficult to analyze the dose dependence of the different implant directions simply by comparing the profile evolutions. Instead, we have

Downloaded 10 Oct 2007 to 150.203.178.60. Redistribution subject to AIP license or copyright, see http://jap.aip.org/jap/copyright.jsp

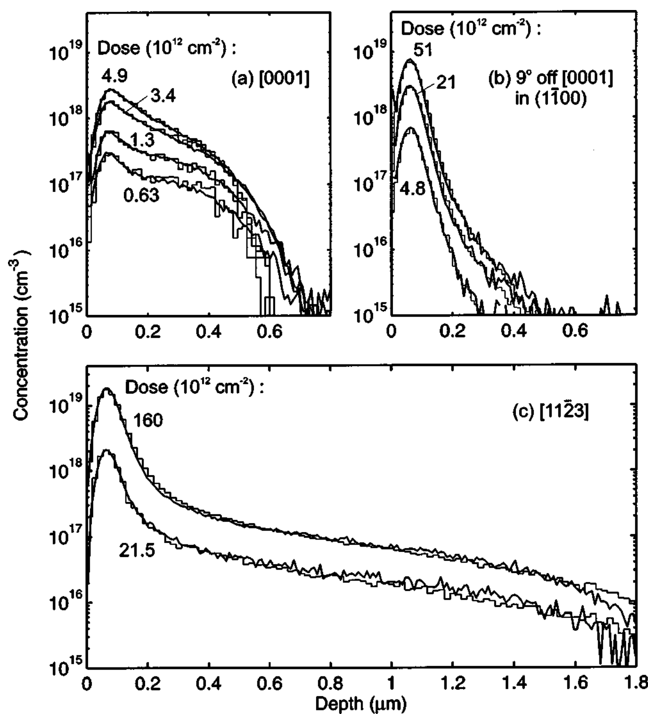

FIG. 4. SIMS (solid lines) and BCA simulated (histograms) profiles of 60 keV Al implantations in 4H-SiC showing different doses for (a) on-axis [0001], (b) 9° tilt from [0001] axis in the $(1\bar{1}00)$ plane, and (c) $[11\bar{2}3]$ direction. The dose dependence was simulated with the c_a parameter of the random scattering model set to (a) 0.6, (b) 0.6, and (c) 0.25.

performed BCA simulations where the influence of crystal damage is treated using a statistical approach where the probability that an ion is randomly scattered by a defect is proportional to the local damage concentration by a constant c_a.[8] With this model good fits were obtained for all implantations, as is demonstrated in Fig. 4, but different values of c_a were obtained for the different implantation directions. For example, a more than two times higher c_a was extracted for the [0001] implanted sample [Fig. 4(a)] compared to $[11\bar{2}3]$ [Fig. 4(c)]. The differences observed in the extracted c_a parameters indicate that the interstitial defects are not randomly distributed as assumed in the simulations, but have fixed positions in the lattice and therefore affect the ions differently in different crystal channels. It may, therefore, be possible to gain information of the position of the defects in the crystal from this data, using a more refined model for dechanneling in the BCA simulations. Further, a directional dependence of the formation and dynamic annealing of these defects cannot be excluded. In this context, it is also interesting to note that a very similar value for c_a was obtained for the present 60 keV Al [0001] implant in 4H-SiC as for the 1.5 MeV [0001] Al implants in 6H-SiC presented in Ref. 8. More details about the simulations and the dose dependence of these implantations will be presented elsewhere.[11]

IV. CONCLUSION

In summary, we have studied the range profiles of 60 keV Al^- implanted in various axial, planar, and random directions of 4H-SiC. For the (0001) wafers, tilting along the $(1\bar{1}00)$ plane did not result in significant planar channeling in contrast to tilting along the $(11\bar{2}0)$ plane. The $[11\bar{2}3]$ axis was also shown to be a significant axial channel extending approximately twice as deep as the implant along [0001]. For the $(11\bar{2}0)$ wafers, a 10° tilt along various planes around the main crystallographic axis resulted in the largest degree of channeling along the (0001) plane with no planar channeling observed for the implant in the $(1\bar{1}00)$ plane. Deepest channeling was observed for the $[11\bar{2}0]$ direction where the deepest channeled ions penetrated 45 times deeper than the projected range of a corresponding random implant. These results can be used as a guide in the choice of implantation direction in order to minimize channeling, and as standards to be used in the development of ion implantation simulators.

ACKNOWLEDGMENTS

The authors are grateful to Professor J. S. Williams for invaluable discussions, Dr. A. P. Byrne (Nuclear Physics), and Tony Watt for hardware used in this project. The authors acknowledge the STINT (Swedish Foundation for international cooperation in research and higher education) program and Australian Research Council for support under the Discovery grant and fellowship program.

[1] *www.cree.com.*
[2] *www.sterling-semiconductor.com.*
[3] E. Albertazzi and G. Lulli, Nucl. Instrum. Methods Phys. Res. B **120**, 147 (1996).
[4] S. Ahmed, C. J. Barbero, T. W. Sigmon, and J. W. Erickson, J. Appl. Phys. **77**, 6194 (1995).
[5] E. Morvan, P. Godignon, M. Vellvehi, A. Hallén, M. Linnarsson, and A. Y. Kuznetsov, Appl. Phys. Lett. **74**, 3990 (1999).
[6] E. Morvan, N. Mestres, J. Pascual, D. Flores, M. Vellvehi, and J. Rebollo, Mater. Sci. Eng., B **61–62**, 373 (1999).
[7] E. Morvan, P. Godignon, S. Berberich, M. Vellvehi, and J. Millan, Nucl. Instrum. Methods Phys. Res. B **147**, 68 (1999).
[8] M. S. Janson, A. Hallen, P. Godignon, A. Y. Kuznetsov, M. K. Linnarsson, E. Morvan, and B. G. Svensson, Mater. Sci. Forum **338–342**, 889 (2000).
[9] H. Yano, T. Hirao, T. Kimoto, H. Matsunami, K. Asano, and Y. Sugarawa, IEEE Electron Device Lett. **20**, 611 (1999).
[10] M. S. Janson, siimpl 2002.
[11] M. S. Janson *et al.* (unpublished).

Downloaded 10 Oct 2007 to 150.203.178.60. Redistribution subject to AIP license or copyright, see http://jap.aip.org/jap/copyright.jsp